ORIGINAL ARTICLE

CrossMark

Ground-penetrating radar estimates of tree root diameter and distribution under field conditions

Keitaro Yamase[1] · Toko Tanikawa[2] · Masako Dannoura[3] · Mizue Ohashi[4] · Chikage Todo[1] · Hidetoshi Ikeno[4] · Kenji Aono[5] · Yasuhiro Hirano[6]

Abstract

Key message **Use of ground-penetrating radar (GPR) can non-destructively estimate diameter and distribution of coarse roots in *Cryptomeria japonica* in weathered granite soils under field conditions.**

Abstract Ground-penetrating radar (GPR) has been used as an assessment tool for non-destructive detection of tree root biomass, but few studies have estimated root diameter under forest field conditions. The aim of this study was to clarify whether coarse root diameter of *C. japonica* in weathered granite soils can be estimated using GPR in a forest. Roots of mature *C. japonica* were scanned using a 900 MHz GPR antenna before being excavated. The diameter and distribution of excavated roots were compared with those identified by GPR, and the relationships between the diameter and waveform indices in radar profiles were also examined. The detection frequency of the number of roots larger than 5 mm in diameter was 47.7%. Limiting factors affecting root detection using GPR in forest field conditions were small root diameter, increasing root depth, and number of adjacent roots. Only one waveform index, using the sum of time intervals between zero crossings (ΣT, ns) of all reflection waveforms of GPR within the range from the first break time at the root top to the delay point time at the root bottom, had a significant relationship with excavated root diameters. A linear regression model was constructed to estimate root diameter using ΣT, and a significant positive relationship in diameter between GPR-estimated and excavated roots was confirmed. The results in this study indicate that the diameter and distribution of *C. japonica* coarse roots under forest field conditions could be estimated using GPR and this technique could contribute to future evaluation of slope stability by evaluating tree roots under vulnerable soils, such as weathered granite.

Keywords Non-destructive root detection · Parabolic waveform · Root diameter · Slope stability · Waveform index

✉ Keitaro Yamase
  kei-yamase@nike.eonet.ne.jp

1 Hyogo Prefectural Technology Center for Agriculture, Forestry and Fisheries, 430 Shiso, Hyogo 671-2515, Japan

2 Kansai Research Center, Forestry and Forest Products Research Institute, Kyoto 612-0855, Japan

3 Graduate School of Global Environmental Studies, Kyoto University, Kyoto 606-8501, Japan

4 School of Human Science and Environment, University of Hyogo, Himeji, Hyogo 670-0092, Japan

5 The General Environmental Technos Co., Ltd. (KANSO Technos), Osaka 541-0052, Japan

6 Graduate School of Environmental Studies, Nagoya University, Nagoya 464-8601, Japan

Introduction

Roots of forest trees play an important role in the mitigation of risk due to natural disasters, such as shallow landslides on mountain slopes (Schwarz et al. 2010). Recently, climate change has altered the intensity and amount of rainfall worldwide (Petley 2010; Chang 2011; Japan Meteorological Agency 2017a), and in Japan is expected to bring an increase in local torrential rainfall (Suzuki et al. 2009; Japan Meteorological Agency 2017a). This means that the importance of tree roots for maintaining slope stability will also increase in mountainous areas in Japan.

Tree roots contribute to slope stability by reinforcement of soil shear strength (Van Beek et al. 2005; Danjon and Reubens 2008; Genet et al. 2008). Several models have been developed to quantify soil reinforcement at the landslide shear plane (Wu et al. 1979; Pollen and Simon 2005;

Springer

Schwarz et al. 2010). These estimates of slope stability are strongly influenced by the diameter and distribution of tree roots (Schwarz et al. 2010), so that information on root size and distribution is essential to utilize such models. However, the acquisition of such root data under field conditions is difficult, since investigations tend to be destructive, laborious, and time-consuming (Reubens et al. 2007; Tobin et al. 2007).

Within the last two decades, the use of ground-penetrating radar (GPR) has attracted root researchers as a non-destructive tool for assessing tree roots in forests (Hruska et al. 1999; Butnor et al. 2001, 2012; Stover et al. 2007; Hirano et al. 2009; Tanikawa et al. 2013). GPR is a broadband electromagnetic pulse radar system that can detect the depth, position, and size of buried materials in soil, using the timing and characteristics of reflected waves (Butnor et al. 2012; Hagrey 2012; Guo et al. 2013a). GPR has successfully been used to estimate tree root biomass in various forest types (Butnor et al. 2001, 2003, 2012, 2016; Stover et al. 2007; Samuelson et al. 2008, 2014; Hirano et al. 2012; Borden et al. 2014, 2016; Bain et al. 2017). GPR has also been used for estimating the diameter and position of individual roots under experimentally controlled conditions (Barton and Montagu 2004; Cui et al. 2011; Tanikawa et al. 2013, 2014; Guo et al. 2015), in a shrub in sandy soils (Wu et al. 2014), and most recently in an agricultural wheat crop field (Liu et al. 2018). However, few studies have estimated the diameter of tree roots under forest field conditions.

The intensive rain that fell in 2014 in the Hiroshima Prefecture in Japan caused a serious landslide disaster, where many shallow small-scale landslides occurred over weathered granite soils (Chigira et al. 2011; Tsuchida et al. 2016). In Japan, such soils occur frequently and often support coniferous forest plantations of such species as *Cryptomeria japonica* (L.f.) D. Don. Therefore, an urgent evaluation of how landslides could be mitigated by these forests, and a management protocol for such plantations that does not just focus on timber production, but is also designed to prevent soil erosion and landslides, are needed. GPR is a technique that shows potential for a non-destructive evaluation of the diameter and distribution of tree coarse roots in weathered granite soils. If it is possible to estimate root reinforcement of soil using GPR, it will drastically enhance the development of forest management techniques to increase root reinforcement, and to mitigate landslide disasters.

Under experimentally controlled conditions, it has been found that several factors, such as the water content of roots and soils, root depth, and root growth direction, limit the detection of tree roots with GPR (Dannoura et al. 2008; Hirano et al. 2009; Cui et al. 2011, 2013; Guo et al. 2013a, b, 2015; Tanikawa et al. 2013, 2016; Bain et al. 2017). However, few studies have examined whether these limiting factors affect tree root detection, or the estimation of root diameter, under forest field conditions. The only study under field conditions we found was of *Pinus thunbergii* stands in a sandy soil, and a decrease of root detection was reported with an increase in rooting depth (Hirano et al. 2012). This was attributed to the attenuation of GPR wave energy.

The final goal of this study was to use GPR to estimate *C. japonica* root diameter and distribution in weathered granite soils on a mountain slope. The specific goals of this paper were: (1) to clarify whether previously proposed limiting factors, such as diameter, depth, and density of roots, affect the detection of roots by GPR, and (2) to identify which GPR waveform index is the most suitable for estimating the *C. japonica* root diameter in weathered granite soils in a mountain area.

Materials and methods

Study site

This study was conducted in a 43-year-old *C. japonica* plantation stand, at the Futatabi park in Rokko mountain, Kobe, Hyogo, Japan (34°43′N, 135°10′E, 430 m a.s.l.). *C. japonica* is one of the main commercial forest species in Japan, comprising 18% of the total forested area (Forestry Agency of Japan 2012). The stand density and basal area of *C. japonica* were 900 trees ha^{-1} and 77 m^2 ha^{-1}, respectively, and understory species such as *Eurya japonica* and *Pleioblastus argenteostriatus* f. *glaber*, were also present. The mean height (H) and stem diameter at breast height (DBH) of *C. japonica* trees were 21.1 m and 32.9 cm, respectively. At the nearest meteorological station, Kobe (34°42′N, 135°13′E, 5 m a.s.l.), the mean annual temperature and precipitation over the past 30 years were 16.7 °C and 1216 mm, respectively (Japan Meteorological Agency 2017b). The soil type was classified as brown forest soil (Forest Soils Division 1976) and a Cambisol (FAO-UNESCO 1994). This soil consisted mainly of weathered granite, which was common in this area.

Radar investigation

In May 2014, two mature *C. japonica* trees were selected, because they had representative growth of H and DBH among trees in the stand. The H of each tree was 21.1 m (Tree No. 1) and 21.9 m (Tree No. 2). The DBH of each tree was 32.9 cm (Tree No. 1) and 36.9 cm (Tree No. 2). A 4×4 m square plot was centered around each tree (Fig. 1). Within the plot, six concentric transects for GPR scanning were established at 25 cm intervals, from 50 to 175 cm, around each stem (Fig. 2). The litter and aboveground parts of any groundcover plants (e.g., mosses and grasses) on the forest floor were removed, because they could affect
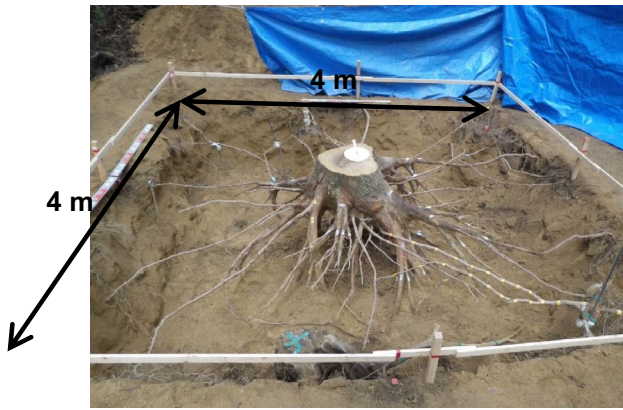
Fig. 1 Coarse root system of one of the mature *Cryptomeria japonica* trees assessed (Tree No. 1), after GPR scanning and excavation within a 4×4 m area

the detection accuracy of roots in a GPR survey (Tanikawa et al. 2016).

GPR scanning for this study was conducted using a field-portable system with a 900 MHz antenna (SIR SYSTEM 3000; Geophysical Survey Systems, Inc, Nashua, NH, USA); the device had a bow-tie dipole configuration. The antenna was calibrated for gains at five points: − 5, 7, 14, 20 and 35 dB. After the leveling of ground surfaces, a polyethylene sheet of 4 ×4 m, within which the six concentric transects were described, was set on the ground around each tree stem to maintain smooth soil surfaces for GPR scanning. In the deployment, the radar equipment was placed on a sled to keep parallel to the ground surface, and a stable scan was made slowly at a relatively constant speed. The dimension and shape of the GPR delivery could play an important role in root detection, in particular under forest field conditions. During the GPR scanning of the concentric transects, the position was marked manually at 15° intervals. Even when the scanning speed was not constant, the position of transects could be corrected at equal distances between the markers. Radar profiles were collected in 8-bit files with a range of 15 ns along each concentric transect. After scanning, 100 cm^3 soil cores were collected at depths of 0–10 and 20–30 cm, to measure the volumetric soil water content at three points within the scanned plots. Soil samples were oven-dried at 105 °C for 24 h. The volumetric water contents at depths of 0–10 and 20–30 cm in the weathered granite soil were 37.9 ± 2.3 and $26.9 \pm 6.5\%$, respectively [$n = 3$, mean ± standard deviation (SD)].

Root excavation

After scanning the concentric transects, root systems of both *C. japonica* trees were excavated from the plots, to a depth of 100 cm, using an air spade. The air spade sprayed compressed air, to blow off the soil and expose the root
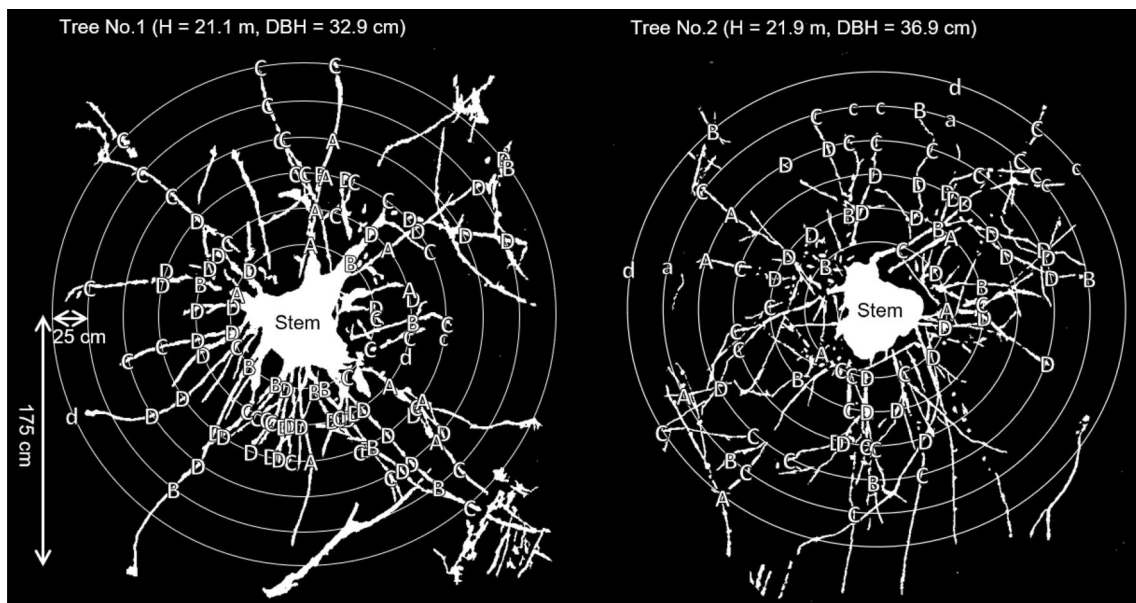

Fig. 2 Bird's eye images of excavated root systems of *C. japonica* trees showing the horizontal positions of roots detected with GPR. Concentric circles show transects for GPR scanning, and letters indicate horizontal root positions and radar reflection waveforms of detected roots. Lower case letters indicate the positions, where the bird's eye images were not acquired because of inadequate excava-tion (but which were excavated and measured later). Radar reflection waveforms were categorized as the following four types, as defined by Cox et al. (2005): **A** strong contrast amplitude and well-defined parabolic, **B** poor contrast amplitude and well-defined parabolic, **C** strong contrast amplitude and slight curvature, **D** poor contrast amplitude and slight curvature

systems (Fig. 1). In the previous studies on the estimation of root diameter, the minimum diameter for detectable roots was found to be 5 mm, using 1500 MHz or 2000 MHz GPR (Butnor et al. 2001; Cui et al. 2011). Therefore, all roots with less than a 5 mm diameter were removed. A bird's eye photo of each plot was obtained thereafter by photographing the ground surface with a digital camera (HERO3+, GoPro Inc., San Mateo, CA, USA) from 5 m above and binarized to extract an image of the isolated excavated root system to visualize clearly. The image was extracted manually using segmentation software (ITK-SNAP, ver. 3.2) (Yushkevich et al. 2006; Ohashi et al. 2016). The positions of coarse roots (> 5 mm in diameter) were measured under the concentric transects in the field. For roots positioned horizontally, both the distance from the center of the stem, and the direction at 1° intervals clockwise from magnetic north, were measured. For roots positioned vertically, the depth from the ground surface before the excavation was measured in 1 cm units. The root diameter was measured in 0.1 mm units, using a digital caliper. In addition, we measured the angle any coarse root subtended to the concentric transect lines, because root detection using GPR has been shown to be affected by the angle between root growth and the scan direction (Tanikawa et al. 2013). Ten roots of different diameters (6.5–84.0 mm) and lengths (5.8–11.3 cm) were sub-sampled from both trees. The root samples were oven-dried at 80 °C for 3 to 4 days until constant weight and volumetric water contents were calculated; these ranged from 69.3 to 91.8% (80.3 ± 7.0%, $n = 10$, mean ± SD).

Data processing

Normalization and filtration of radar diagrams were performed using RADAN (for Windows, Geophysical Survey Systems). The parallel reflections from the ground surface and soil horizons were eliminated by applying a background-removal filter (Butnor et al. 2003). Since the reflected waveform is governed by the difference in relative permittivity of substances and varies depending on the volumetric water content of the soil (Hagrey 2012), the soil dielectric constant was set to 9.0 (dimensionless), based on the reflected waveform of a steel pipe buried at a known depth (soil depth = 30 cm). Since the detectable angles between root growth and radar scanning range from 45° to 135° (Tanikawa et al. 2013), the positions of excavated roots following these angles were noted and compared with those identified from the radar image under forest field conditions. The manual input of the position markers at 15° intervals, and changes in root positions during the air spade removal of surrounding soils, might have resulted in errors in root positions. Therefore, we defined that roots were "detected" using GPR when the excavated

roots existed within a 10 cm radius of the root positions identified using GPR.

Roots were identified manually by GPR according to where hyperbolas of radar reflection waveforms were observed compared to the surrounding areas (Hirano et al. 2009). We categorized signals of radar reflection waveforms, which potentially correspond to root traces, into the following four types, as defined by Cox et al. (2005):

Waveform A: having contrasting bands of high amplitude and a well-defined parabolic shape,
Waveform B: having poor amplitude contrast, but a well-defined parabolic shape,
Waveform C: having contrasting bands of high amplitude, but only slight curvature,
Waveform D: having poor amplitude contrast and slight curvature.

The horizontal position and types of waveform signal of detected roots were overlapped with the extracted root system image to evaluate which roots were detected by GPR.

We used two main GPR indices, T (time interval between zero crossing) and A (amplitude area) of reflection waveforms within the range from the first break time at the root top to the delay point time at the root bottom, and calculated the sum or maximum values of each index as defined by Tanikawa et al. (2013) (Fig. 3).

ΣT: sum of time intervals between zero crossing for all of reflection waveforms (ns), single T_{max}: time interval between zero crossing of the maximum reflection waveform (ns), ΣA: sum of amplitude areas for all of the reflection waveforms (dB × ns), single A_{max}: amplitude area of the maximum reflection waveform (dB × ns).

Hirano et al. (2009) reported that two coarse roots were not recognized as different individual roots when the intervals between neighboring roots were less than 20 cm, using 900 MHz GPR, under optimal sandy soil conditions. Therefore, the numbers of excavated coarse roots adjacent (within a 20 cm interval) to the target were also recorded in the present study.

Statistical analysis

To clarify factors that determine the success or failure of root detection, a generalized linear mixed model (GLMM), with a binomial distribution and a logit link function was used. The explanatory variables were root diameter, root depth, and the number of roots adjacent to the target root, while the random effect was the tree-specific effect for individual *C. japonica* trees. Akaike's information criterion (AIC) was used to compare the relative quality of the models, and the model with the minimum AIC was selected as the best-fit estimator. To determine which waveform indices were suitable for

Fig. 3 Representative 900 MHz radar profile and extraction of the radar wave parameters (modified from Tanikawa et al. 2016). **a** Representative reflected hyperbola in a radar profile of a root at a depth of 23 cm; **b** reflection waveforms and the four waveform parameters extracted in this study
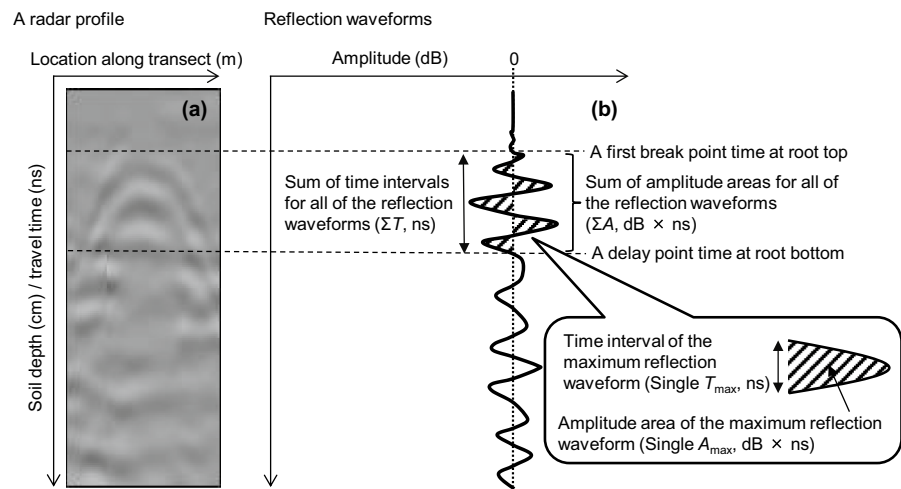
the estimation of root diameter, regression analysis between the measured values of root diameter by excavation, and the GPR waveform indices, was attempted using linear, exponential, power and logistic forms. The regression equation with the minimum AIC was also selected. All statistical analyses were conducted using the R 3.4.2 statistical package (R Core Team 2017).

Results

Limiting factors to GPR-based coarse root detection

We excavated a total of 427 roots that were > 5 mm in diameter, under 12 concentric transects around two *C. japonica* trees; 388 roots had radar-detectable angles from 45° to 135° between root growth and radar scanning. From the 388 roots following detectable angles (defined as "target roots" in this study), GPR detected 185 roots as hyperbolas in radargrams (Figs. 2, 4), and thus the detection frequency of roots (i.e., the ratio of the number of roots detected using GPR to the number of target roots) was 47.7%. Generalized linear mixed model analysis selected Model 1 (Table 1) using only three variables without interactions as the best fit model with the lowest AIC value (507.2) among all possible models using three variables and their interactions. Each of three variables, root diameter, root depth, and number of adjacent roots (root density) all significantly affected root detection by GPR (Table 1, GLMM, $P < 0.01$ for root diameter, $P < 0.001$ for root depth and root density), indicating that these were limiting factors for detection under forest field conditions. The mean diameter of roots detected using GPR was 31.1 ± 38.2 mm (mean $\pm$ standard deviation), and that of undetected roots was 23.2 ± 22.7 mm (Table 2a). The mean depths of detected and undetected roots were

20.4 ± 16.8 and 25.9 ± 21.7 cm, respectively (Table 2b). The mean numbers of roots adjacent to the target root that were detected and undetected were 1.3 ± 1.4 and 1.7 ± 1.8, respectively (Table 2c). In fact, isolated roots were more frequently detected than densely positioned roots (Fig. 2). The estimates of detection frequency of roots using GPR by GLMM regression analysis showed that the ratio increased with increasing root diameter, whereas the ratio decreased with increasing root depth and number of adjacent coarse roots (Fig. 5). The concordance ratios of the number of target roots detected and undetected, to the response variable values predicted by the best-fitted model, were 28.1 and 34.0%, respectively (Table 3).

Suitable GPR waveform indices for estimating root diameter

To determine which GPR waveform indices among the four proposed (ΣT, Single T_{max}, ΣA, Single A_{max}), were most suitable for estimating root diameter under these forest field conditions, the relationships between the diameter of detected roots and each GPR index were analyzed. When waveforms A and B, which had well-defined parabolic shapes, were considered ($n = 41$), only one index, ΣT, was correlated significantly with root diameter (Fig. 6, $R^2 = 0.48$, $P < 0.001$). However, no significant correlations were found between root diameter and ΣT (nor with the other three indices) in waveforms C and D, which showed only slight curvature traces (data not shown, $n = 144$, $P > 0.05$).

Estimation accuracy of root diameter

We measured the positions of 185 roots detected using GPR and could estimate the diameter of 41 roots for which the shapes of waveforms A and B were observed (Fig. 2). To apply the relationship between diameter (*D* mm) of 41
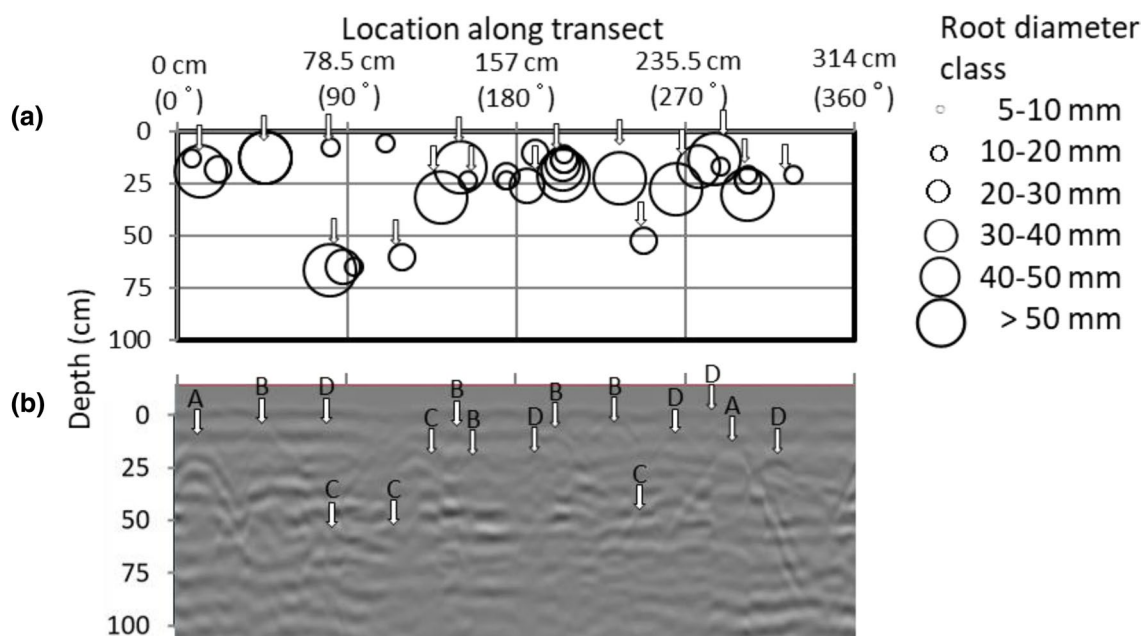
Fig. 4 **a** Spatial distribution of *C. japonica* roots, and **b** GPR images of roots in a representative concentric transect at a 50 cm distance from the stem (Tree No. 1). Circles in the vertical soil profile (**a**) and the hyperbolas in the GPR images (**b**) identify root positions. White excavated roots and arrows indicate roots that were detected by GPR. Letters show classification of the four types of waveforms as defined by Cox et al. (2005) (see Fig. 2)

excavated roots and ΣT (ns) of waveforms A and B, the linear regression with the minimum AIC was selected, and the following regression equation was obtained (Fig. 6);

$$\Sigma T = 0.02D + 3.34 \left(R^2 = 0.48, P < 0.001, n = 41 \right).$$

As for the linear regression, the data on the largest root diameter ($D = 265$ mm) might affect the relationship. However, the regression equation excluding this data exhibited $\Sigma T = 0.02D + 3.32$ ($R^2 = 0.35$, $P < 0.05$, $n = 40$, the dashed line of Fig. 6), indicating that the relationships, irrespective of this data are quite similar. By applying the ΣT values of waveforms A and B for 41 roots with this regression equation, a significant positive relationship was found between the estimated values of the roots detected using GPR and the actual diameter of roots measured by excavation (Fig. 7, $R^2 = 0.48$, $P < 0.001$).

Discussion

Estimation of tree root diameter with GPR

In this study, we succeeded in estimating the diameters of mature *C. japonica* roots using a waveform index of GPR, ΣT, in a mountainous forest standing over weathered granite soils. The methods for estimating root diameter from reflection waveform indices of GPR have been developed in the previous studies, mostly using experimentally controlled conditions, and some controlled experiments were even done in the field (Barton and Montagu 2004; Cui et al. 2011, 2013; Tanikawa et al. 2013, 2014, 2016). However, this study has demonstrated an application of this technique in forests, where soil structure and condition are highly heterogeneous. The non-destructive estimates of diameter and distribution of coarse roots using GPR would enable us to use the models for evaluating root reinforcement, because spatial distribution, diameter, and number of roots are essential inputs (Wu et al. 1979; Pollen and Simon 2005; Schwarz et al. 2010). The estimates of root reinforcement could provide a basis to support forest management actions, such as adjusting tree density to prevent shallow landslides caused by torrential rainfall (Japan Meteorological Agency 2017a). However, further trials of GPR in other forest types and soils are needed to advance the practical use of this technique for root detection.

GPR waveform indices for estimating root diameter under forest field conditions

The results of this study revealed that the reflection waveform parameter ΣT was the only suitable index among the four proposed for estimating root diameter under forest field conditions (Fig. 4). The previous studies have clarified that two indices concerning GPR reflection time,

Table 1 Statistics of the Akaike information criterion (AIC) for the top five selected generalized linear mixed models (GLMM) among all possible models using three variables, root diameter (diameter), root depth (depth), and number of adjacent roots (density) for explaining GPR detected/undetected roots

Response variable	Explanatory variables included in model	AIC	Estimate	SE	P
Detected (1)/undetected (0) root	Model 1: diameter	507.2	0.012	0.004	< 0.010
	Depth		− 0.019	0.006	< 0.001
	Density		− 0.344	0.077	< 0.001
	Model 2: diameter	507.3	0.005	0.006	0.370
	Depth		− 0.019	0.006	< 0.001
	Density		− 0.472	0.124	< 0.001
	Diameter × density		0.004	0.003	0.180
	Model 3: diameter	508.1	0.005	0.006	0.460
	Depth		− 0.024	0.007	< 0.010
	Density		− 0.573	0.158	< 0.001
	Diameter × density		0.005	0.003	0.131
	Depth × density		0.006	0.005	0.275
	Model 4: diameter	509.8	0.007	0.008	0.383
	Depth		− 0.021	0.009	< 0.050
	Density		− 0.577	0.159	< 0.001
	Diameter × depth		− 0.001	0.001	0.592
	Diameter × density		0.006	0.005	0.251
	Depth × density		0.005	0.003	0.160
	Model 5: diameter	511.8	0.001	0.001	0.382
	Depth		− 0.020	0.011	0.074
	Density		− 0.561	0.188	< 0.010
	Diameter × depth		− 0.000	0.000	0.620
	Diameter × density		0.004	0.004	0.330
	Depth × density		0.005	0.009	0.580
	Diameter × depth × density		0.000	0.000	0.880

GLMM analysis selected Model 1 using only three variables without their interactions as the best-fit model with the lowest AIC value (507.2) and showed each of the three variables all significantly affected detection in Model 1 ($P < 0.01$)

Single T_{max} (time interval between zero crossings of the maximum waveform), and ΣT (sum of the time intervals), were not affected by several limiting factors for root detection, such as the water content of roots, the angles between root growth and GPR scanning, and the litter thickness of surface soils (Cui et al. 2011, 2013; Guo et al. 2013b; Tanikawa et al. 2013, 2014, 2016). The waveform indices for root detection in GPR images such as intensity or amplitude, are susceptible to these limiting factors. On the other hand, the time interval at zero amplitude of the reflection waveform indicates the time when the reflected wave is emitted from the root and is not greatly influenced by the factors for changing the amplitude (Cui et al. 2011, 2013; Guo et al. 2013b; Tanikawa et al. 2013, 2014). Barton and Montagu (2004) first proposed that the use of an index relating to time intervals could be used to estimate root diameter under experimental conditions, and they used only a time interval of a half waveform such as Single T_{max}. Later, Cui et al. (2011) showed that ΣT, the time interval for the radar-reflected waves to reach the top and bottom of roots,

could be an index for estimating root diameter under model conditions. Tanikawa et al. (2013) clarified that ΣT was the most suitable indicator among the four proposed indices, and even better than Single T_{max}, presumably because Single T_{max} was only a half waveform without considering other reflected waveform. ΣT has the major advantage of indices, because it only depends on the geometric dimension of the reflector and is independent of signal strength (Cui et al. 2011). This study confirmed, under forest field conditions, that ΣT could be a useful index for estimating tree roots diameters. Although the ranges in root diameter estimated in the previous experiments were narrower, such as 0–40 mm (Cui et al. 2011) and 20–80 mm (Barton and Montagu 2004; Tanikawa et al. 2013), we were able to estimate wider ranges, from 5 to 265 mm, for mature *C. japonica* roots under forest field conditions, suggesting that this method can be more practical for *in situ* ranges of tree root diameter.

The other two indices relating to the amplitude area of the reflection waveform, Single A_{max} (amplitude area of the

Table 2 Number of *Cryptomeria japonica* roots detected or undetected by GPR (a) by different root diameter classes, (b) at different root depths, and (c) with different numbers of adjacent roots

(a) Root diameter

Root diameter (mm)	Number of GPR detected/undetected roots (no.)						Mean ± SD (mm)
	5–50	50–100	100–150	150–200	200–250	250–300	
Detected (*n* = 185)	156	20	5	1	2	1	31.1 ± 38.2
Undetected (*n* = 203)	186	15	1	0	1	0	23.2 ± 22.7
Detection frequency (%)	45.6	57.1	83.3	100	66.7	100	

(b) Root depth

Root depth (cm)	Number of GPR detected/undetected roots (no.)						Mean ± SD (cm)
	0–15	15–30	30–45	45–60	60–75	75–90	
Detected (*n* = 185)	88	51	20	20	6	0	20.4 ± 16.8
Undetected (*n* = 203)	80	55	23	22	20	3	25.9 ± 21.7
Detection frequency (%)	52.4	48.1	46.5	47.6	23.1	0	

(c) Number of adjacent roots (root density)

Number of adjacent roots (no.)	Number of GPR detected/undetected roots (no.)										Mean ± SD (no.)
	0	1	2	3	4	5	6	7	8	9	
Detected (*n* = 185)	57	72	37	05	6	3	3	1	0	1	1.3 ± 1.4
Undetected (*n* = 203)	54	66	43	13	5	9	6	7	0	0	1.7 ± 1.8
Detection frequency (%)	51.4	52.2	46.3	27.8	54.5	25.0	33.3	12.5	–	100	

Mean values are shown for (a) root diameter, (b) root depth, and (c) number of adjacent roots, for GPR detected or undetected roots

maximum reflection waveform) and Σ*A* (sum of the amplitude areas), are influenced by the proposed limiting factors (Cui et al. 2011; Guo et al. 2013a; Tanikawa et al. 2013, 2014, 2016). In this study, GPR scanning on concentric transects was carried out, and there were several directions of roots that had 0-130° angles between root growth and radar scanning, suggesting that the angles between the scanning and roots could affect the two amplitude indices. The variation in root water content was likely to create differences in these two indices, as pointed out by the previous studies (Hirano et al. 2009; Guo et al. 2013a). Guo et al. (2013a) suggested that appropriate GPR indices and regression models should be selected based on the water content range of roots, because the amplitude area of the reflection waveform changed greatly at different root water content levels even though root size is the same. However, this study was not

able to establish a model using either of these area indices that would enable field estimation of root diameter. Butnor et al. (2001) showed that GPR resolution, i.e., the amplitude of waveform, was best in the sandy soils but degraded in soils with high water and clay contents. Future studies are needed to clarify the degree of the suitability of GPR indices in different soil conditions and forest types in field conditions.

Factors affecting root detection in the field

In this study, the detection frequency of numbers of roots using GPR was 47.7% among the target roots (> 5 mm diameter) using GPR detectable angles under the concentric transects. Limiting factors affecting root detection were root diameter, root depth, and the numbers of adjacent
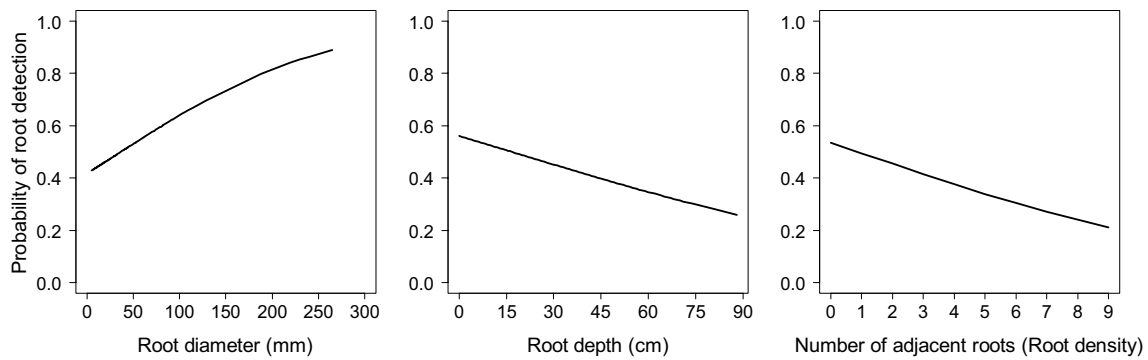
Fig. 5 Effect of root diameter, root depth, and number of adjacent roots to the target root, on the probability of root detection in *C. japonica*. The probability was 1 (detected by GPR) or 0 (undetected by GPR). The solid lines show the fitting values obtained by the selected model (Table 1)

Table 3 Numbers of GPR detected or undetected roots by value of response variable expected by the best fitted model

Number of roots (no.)	Expected value of response variable (*E*)	
	Undetected (*E* ≤ 0.5)	Detected (*E* > 0.5)
Detected root (1)	76 (19.6%)[a]	109 (28.1%)[a]
Undetected root (0)	132 (34.0%)[a]	71 (18.3%)[a]

[a]The values in parentheses show the percentage of detected or undetected roots amongst the total of 388 targeted roots

roots; large diameter roots were most easily detected followed by those at shallower depths, and those with fewer adjacent roots (Fig. 4). The concordance ratio of the number of roots, using the best fitted model, was 62.1% for the total of detected (28.1%) and undetected (34.0%) roots (Table 3). Under sandy soil conditions, using 1500 MHz GPR in a *P. thunbergii* forest, the detection frequency for numbers of roots in the 5–10 mm diameter class was only 6.6%, whereas 54% of roots that were larger than 10 mm were detected (Hirano et al. 2012). This could support the results of a detection frequency of 47.7% for *C. japonica* roots in our study. Although the detectable horizontal angles were considered in our study, the lower frequency might be caused by unconsidered limiting factors, such as more heterogeneous soil conditions compared to sandy soils, the angle in the vertical direction (Liu et al. 2017), and the accumulation of fine roots. Fine root biomass in *C. japonica* is generally higher than that in *P. thunbergii* (Noguchi et al. 2007) and the accumulation of fine roots could cause large variation in the reflected electromagnetic waves in the surface soils, similar to the effects of leaf litter thickness (Tanikawa et al. 2016). In the future, the effects of these limiting factors on the detection frequency should be clarified. In contrast, our results suggest that estimating thicker coarse roots could be advantageous for the evaluation of slope stability, because thicker roots contribute more to slope reinforcement (Wu et al. 1979; Pollen and Simon

2005; Schwarz et al. 2010). Therefore, a non-destructive evaluation using GPR of the contribution of coarse roots to slope stability could be made.

Our findings also support the previous experimental results on the effects of depth and density of roots on GPR root detection (Hirano et al. 2009; Cui et al. 2011, 2013). Since the electromagnetic pulses emitted into the ground attenuate with increasing soil depth, and even if roots are thicker, deeper roots are only detected as small intensities of reflected waveforms (Cui et al. 2011, 2013). Hirano et al. (2009) pointed out that the GPR waveforms were not individually determined for two *C. japonica* roots at intervals of 20 cm, using 900 MHz in sandy experimental conditions. The results from this study also indicated that the number of adjacent roots was a limiting factor for root detection. The existence of adjacent roots could cause mutual interference of reflected waveforms, and decrease the number of waveforms in the radargram. Butnor et al. (2016) have recently shown that the detection frequency of tree root biomass was consistently lower in the vicinity of the stem because of dense rooting, and this was true for the detection and diameter estimation of roots in our study (Fig. 2). The present study showed the number of accurate GPR estimates for coarse diameter roots in mature *C. japonica* was still limited to 41 roots among 185 detected roots, out of 388 targeted roots. To raise the detection frequency using GPR, we need to scan other types of transects, such as grid survey lines, consider different scan angles (Tanikawa et al. 2013; Guo et al. 2015; Bain et al. 2017; Liu et al. 2017), and set the transects at appropriate distances from the stem because of the lower root density (Butnor et al. 2016). Parallel survey lines of GPR between tree stems have been used for extensive investigation of estimates of root biomass in forest stand scales (Butnor et al. 2001, 2003). Continuous regions of weak reinforcement are expected to be prone to failure and may contribute to the risk of landslide occurrence (Schwarz et al. 2010). The points at the middle distances
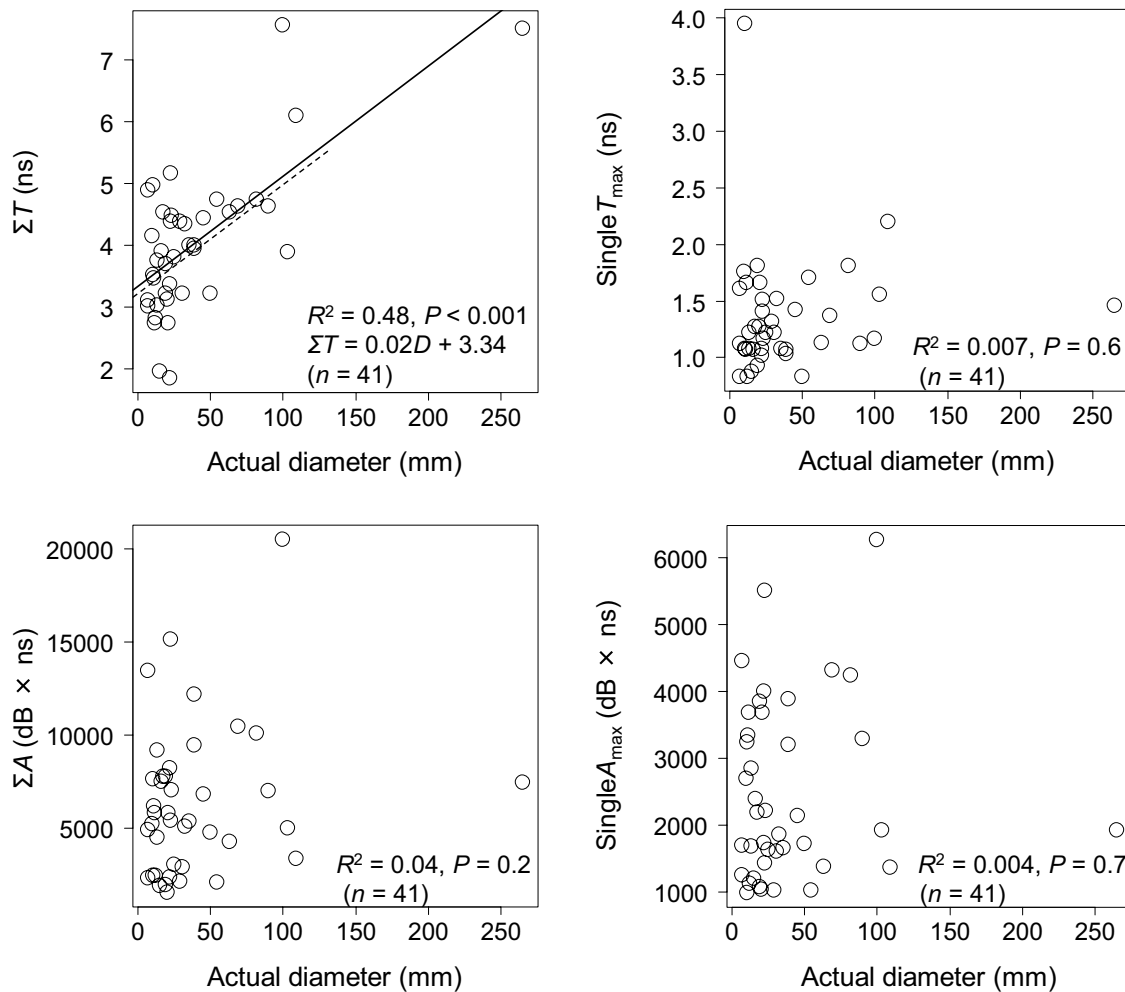
Fig. 6 Relationships between four GPR waveform indices of the reflected waveforms A and B, which had well-defined parabolic shapes, and actual diameters of excavated roots. The solid line shows the linear regression using all data ($n=41$) between GPR wave-form index ΣT and actual root diameters. The dashed line shows the linear regression excluding the data on the largest root diameter ($D = 265$ mm), and the equation is as follows; $\Sigma T = 0.02D + 3.32$ ($R^2 = 0.35$, $P < 0.05$, $n = 40$)

between tree stems could show the lowest reinforcement for landslide, and thus, parallel survey lines in these areas could obtain information on the vertical distribution and diameter of tree roots for estimates of slope stability in forest stand scales. Further trials for estimates of root reinforcement using parallel survey lines at stand scales are needed to enhance the utility of root detection using GPR for proposing management protocols of forest plantations.

Conclusion

This is the first study to show that a GPR waveform index, ΣT (sum of the time intervals between zero crossings), can estimate the root diameter of mature *C. japonica* trees in weathered granite soils under forest field conditions, even though there has been extensive experimental evidence

suggesting this possibility. The study confirmed the impact of previously proposed limiting factors, such as root diameter, root depth, and root density on root detection using GPR under forest field conditions. Forested areas on granite soils are well-known for having frequent shallow landslides (Chigira et al. 2011). Therefore, we need to estimate the slope stability in these forest soils, including root reinforcement. As results from this study have shown, nondestructive estimates of root diameter distribution in upper layers of soil with GPR could contribute to the evaluation and management of slope stability under forest field conditions, particularly for less resilient soils such as granite.

Author contribution statement KY: planned, performed the experiment, conducted data analyses, wrote the paper and prepared the manuscript for submission; TT: planned, performed the experiment and the data analyses, MD: planned
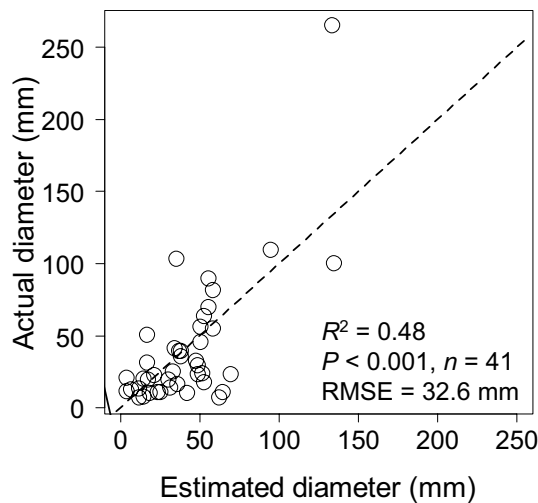
Fig. 7 Measured root diameters (from excavated roots) were plotted against the root diameter estimated by fitting a linear regression model, based on data from the GPR waveform index ΣT. The dashed line shows the 1:1 relationship

and performed the experiment; MO: conducted data analyses and wrote the paper; CT: planned and performed the experiment and the data analyses; HI: planned and performed the experiment and the data analyses; KA: performed the experiment and the data analyses; YH: planned, performed the experiment, conducted data analyses, wrote and edited the paper.

Compliance with ethical standards

Conflict of interest The authors declare that they have no conflicts of interest.

References

Bain JC, Day FP, Butnor JR (2017) Experimental evaluation of several key factors affecting root biomass estimation by 1500 MHz ground-penetrating radar. Remote Sens 9:1337. https://doi.org/10.3390/rs9121337

Barton CV, Montagu KD (2004) Detection of tree roots and determination of root diameters by ground penetrating radar under optimal conditions. Tree Physiol 24:1323–1331. https://doi.org/10.1093/treephys/24.12.1323

Borden KA, Isaac ME, Thevathasan NV, Gordon AM, Thomas SC (2014) Estimating coarse root biomass with ground penetrating radar in a tree-based intercropping system. Agroforest Syst 88:657–669. https://doi.org/10.1007/s10457-014-9722-5

Borden KA, Thomas SC, Isaac ME (2016) Interspecific variation of tree root architecture in a temperate agroforestry system characterized using ground-penetrating radar. Plant Soil 410:323–334. https://doi.org/10.1007/s11104-016-3015-x

Butnor JR, Doolittle JA, Kress L, Cohen S, Johnsen KH (2001) Use of ground-penetrating radar to study tree roots in the southeastern United States. Tree Physiol 21:1269–1278

Butnor JR, Doolittle JA, Johnsen KH, Samuelson L, Stocks T, Kress L (2003) Utility of ground-penetrating radar as a root biomass survey tool in forest systems. Soil Sci Soc Am J 67:1607–1615

Butnor JR, Barton C, Day FP, Johnsen KH, Mucciardi AN, Schroeder R, Sover DB (2012) Using ground-penetrating radar to detect tree roots and estimate biomass. In: Mancuso S (ed) Measuring roots, an updated approach. Springer, Berlin, pp 213–245

Butnor JR, Samuelson LJ, Stokes TA, Johnsen KH, Anderson PH, Gonzalez-Benecke CA (2016) Surface-based GPR underestimate below-stump root biomass. Plant Soil 402:47–62. https://doi.org/10.1007/s11104-015-2768-y

Chang CH (2011) Preparedness and storm hazards in a global warming world: lessons from Southeast Asia. Nat Hazards 56:667–669. https://doi.org/10.1007/s11069-010-9581-y

Chigira M, Mohamad Z, Sien LC, Komoo I (2011) Landslides in weathered granitic rocks in Japan and Malaysia. Bull Geol Soc Malaysia 57:1–6. https://doi.org/10.7186/bgsm2011001

Cox KD, Scherm H, Serman N (2005) Ground-penetrating radar to detect and quantify residual root fragments following peach orchard clearing. Hort Technol 15:600–607

Cui X, Chen J, Shen J, Cao X, Chen X, Zhu X (2011) Modeling tree root diameter and biomass by ground-penetrating radar. Sci China Earth Sci 54:711–719. https://doi.org/10.1007/s11430-010-4103-z

Cui X, Guo L, Chen J, Chen X, Zhu X (2013) Estimating tree-root biomass in different depths using ground-penetrating radar: evidence from a controlled experiment. IEEE Trans Geosci Remote Sens 51:3410–3423. https://doi.org/10.1109/TGRS.2012.2224351

Danjon F, Reubens B (2008) Assessing and analyzing 3D architecture of woody root systems, a review of methods and applications in tree and soil stability, resource acquisition and allocation. Plant Soil 303:1–34. https://doi.org/10.1007/s11104-007-9470-7

Dannoura M, Hirano Y, Igarashi T, Ishii M, Aono K, Yamase K, Kanazawa Y (2008) Detection of *Cryptomeria japonica* roots with ground penetrating radar. Plant Biosyst 142:375–380

FAO-UNESCO (1994) Soil map of the world, revised legend 1990. World soil resources report 60. FAO, Rome

Forest Agency of Japan (2012) Annual report on forest and forestry in Japan for FY2013. http://www.rinya.maff.go.jp/j/kikaku/hakusyo/23hakusyo/pdf/honbun1-3.pdf Accessed 4 Dec 2017

Forest Soils Division (1976) Classification of forest soils in Japan, vol 280. Bull Gov For Exp Sta, Tokyo, pp 1–28

Genet M, Kokutse N, Stokes A, Fourcaud T, Cai X, Ji J, Mickovski SB (2008) Root reinforcement in plantations of *Cryptomeria japonica* D. Don: effect of tree age and stand structure on slope stability. For Ecol Manag 256:1517–1526. https://doi.org/10.1016/j.foreco.2008.05.050

Guo L, Chen J, Cui X, Fan B, Lin H (2013a) Application of ground penetrating radar for coarse root detection and quantification:

a review. Plant Soil 362:1–23. https://doi.org/10.1007/s1110 4-012-1455-5

Guo L, Lin H, Fan B, Cui X, Chen J (2013b) Impact of root water content on root biomass estimation using ground penetrating radar: evidence from forward simulation and field controlled experiments. Plant Soil 371:503–520. https://doi.org/10.1007/s1110 4-013-1710-4

Guo L, Wu Y, Chen J, Hirano Y, Tanikawa T, Li W, Cui X (2015) Calibrating the impact of root orientation on root quantification using ground-penetrating radar. Plant Soil 395:289–305. https://doi.org/10.1007/s11104-015-2563-9

Hagrey SA (2012) Geophysical imaging techniques. In: Mancuso S (ed) Measuring roots, an updated approach. Springer, Berlin, pp 151–158

Hirano Y, Dannoura M, Aono K, Igarashi T, Ishii M, Yamase K, Makita N, Kanazawa Y (2009) Limiting factors in the detection of tree roots using ground-penetrating radar. Plant Soil 319:15–24. https://doi.org/10.1007/s11104-015-2563-9

Hirano Y, Yamamoto R, Dannoura M, Aono K, Igarashi T, Ishii M, Yamase K, Makita N, Kanazawa Y (2012) Detection frequency of *Pinus thunbergii* roots by ground-penetrating radar is related to root biomass. Plant Soil 360:363–373. https://doi.org/10.1007/s11104-012-1252-1

Hruska J, Cermak J, Sustek S (1999) Mapping tree root systems with ground-penetrating radar. Tree Physiol 19:125–130

Japan Meteorological Agency (2017a) Long-term change in occurrence frequency of torrential rain for a short time. http://www.jma.go.jp/jma/kishou/info/heavyraintrend.html Accessed 11 Dec 2017

Japan Meteorological Agency (2017b) Past weather data. http://www.data.jma.go.jp/obd/stats/etrn/. Accessed 4 Dec 2017

Liu Q, Cui X, Liu X, Chen X, Cao X (2017) Detection of root orientation using ground-penetrating radar. IEEE Trans Geosci Remote Sens 56:93–104. https://doi.org/10.1109/TGRS.2017.2737003

Liu X, Dong X, Xue Q, Leskovar DI, Jifon J, Butnor JR, Marek T (2018) Ground penetrating radar (GPR) detects fine roots of agricultural crops in the field. Plant Soil. https://doi.org/10.1007/s11104-017-3531-3

Noguchi K, Konôpka B, Satomura T, Kaneko S, Takahashi M (2007) Biomass and production of fine rots in Japanese forests. J For Res 12:83–95. https://doi.org/10.1007/s10310-006-0262-3

Ohashi M, Kakizoe T, Ikeno H, Yamase K, Tanikawa T, Dannoura M, Aono K, Todo C, Hirano Y (2016) Detection of horizontal root distribution of a black pine in a sea coast by concentrically searching of ground penetrating radar. J Jpn Soc Reveget Tech 41:385–390 **(in Japanese with English summary)**

Petley D (2010) On the impact of climate change and population growth on the occurrence of fatal landslides in South, East and SE Asia. Q J Eng Geol Hydrogeol 43:487–496. https://doi.org/10.1144/1470-9236/09-001

Pollen N, Simon A (2005) Estimating the mechanical effects of riparian vegetation on stream bank stability using a fiber bundle model. Water Resour Res 41:W07025. https://doi.org/10.1029/2004WR003801

R Core Team (2017) R: a language and environment for statistical computing. T Foundation for Statistical Computing, Vienna Austria. https://www.r-project.org/. Accessed 7 Sep 2017

Reubens B, Poesen J, Danjon F, Geudens G, Muys B (2007) The role of fine and coarse roots in shallow slope stability and soil erosion

control with a focus on root system architecture: a review. Trees 21:385–402. https://doi.org/10.1007/s00468-007-0132-4

Samuelson LJ, Butnor JR, Maier C, Stokes TA, Johnsen K, Kane M (2008) Growth and physiology of loblolly pine in response to long-term response management: defining growth potential in the southern United State. Can J For Res 38:721–732. https://doi.org/10.1139/X07-191

Samuelson LJ, Stocks TA, Butnor JR, Johnson KH, Gonzalez-Beneche CA, Anderson P, Jackson J, Ferrari L, Martin TA, Cropper WP Jr (2014) Ecosystem carbon stocks in *Pinus palustris* Mill. forests. Can J For Res 44:476–486. https://doi.org/10.1139/cjfr-2013-0446

Schwarz M, Lehmann P, Or D (2010) Quantifying lateral root reinforcement in steep slopes—from a bundle of roots to tree stands. Earth Surf Process Landforms 35:354–367. https://doi.org/10.1002/esp.1927

Stover DB, Day FP, Butnor JR, Bert G, Drake BG (2007) Effect of elevated CO_2 on coarse-root biomass in Florida scrub detected by ground-penetrating radar. Ecology 88:1328–1334

Suzuki S, Yoshitake T, Goto Y (2009) Values for forest damage caused by strong wind, heavy rain, snow and forest fire based on statistics compiled in Japan fiscal year 1954 to 2003. Bull FFPRI 8:71–100 **(in Japanese with English summary)**

Tanikawa T, Hirano Y, Dannoura M, Yamase K, Aono K, Ishii M, Igarashi T, Ikeno H, Kanazawa Y (2013) Root orientation can affect detection accuracy of ground-penetrating radar. Plant Soil 373:317–327. https://doi.org/10.1046/j.1365-2745.2002.00682.x

Tanikawa T, Dannoura M, Yamase K, Ikeno H, Hirano Y (2014) Reply to: "Comment on root orientation can affect detection accuracy of ground-penetrating radar". Plant Soil 380:445–450. https://doi.org/10.1007/s11104-014-2136-3

Tanikawa T, Ikeno H, Dannoura M, Yamase K, Aono K, Hirano Y (2016) Leaf litter thickness, but not plant species, can affect root detection by ground penetrating radar. Plant Soil 408:271–283. https://doi.org/10.1007/s11104-016-2931-0

Tobin B, Cermak J, Chiatante D, Danjon F, Di Iorio A, Dupuy L, Eshel A, Jourdan C, Kalliokoski T, Laiho R, Nadezhdina N, Nicoll B, Pages L, Silva J, Spanos I (2007) Towards developmental modelling of tree root systems. Plant Biosyst 141:481–501

Tsuchida T, Moriwaki T, Kumamoto N, Ichii K, Kano S, Nakai S (2016) Investigation of debris flow and damaged areas of 2014 Hiroshima landslide disaster. Jpn Geotech J 11:33–52 **(in Japanese with English summary)**

Van Beek LPH, Wint J, Cammeraat LH, Edwards JP (2005) Observation and simulation of root reinforcement on abandoned Mediterranean slopes. Plant Soil 278:55–74. https://doi.org/10.1007/s11104-005-7247-4

Wu TH, McKinnell WP, Swanston DN (1979) Strength of tree roots and landslides on Prince of Wales Island, Alaska. Can Geotech J 16:19–33

Wu Y, Guo L, Cui X, Chen J, Cao X, Lin H (2014) Ground-penetrating radar-based automatic reconstruction of three-dimensional coarse root system architecture. Plant Soil 282:155–172. https://doi.org/10.1007/211104-014-2139-0

Yushkevich PA, Piven J, Hazlett HC, Smith RG, Sean Ho S, Gee JC, Gerig G (2006) User-guided 3D active contour segmentation of anatomical structures: significantly improved efficiency and reliability. Neuroimage 31(3):1116–1128